JOURNAL OF GUIDANCE, CONTROL, AND DYNAMICS
Vol. 37, No. 3, May–June 2014

Engineering Notes

Negative Collision Measurements in Position/Velocity State Estimation

David K. Geller*
Utah State University, Logan, Utah 84322
and
Yaakov Oshman†
Technion — Israel Institute of Technology, 32000 Haifa, Israel

DOI: 10.2514/1.61820

I. Introduction

A VARIETY of aerospace applications such as orbital rendezvous, powered descent to the surface of a celestial object, aircraft landing, and missile intercept require some form of a desired collision. Other aerospace applications such as orbital satellite inspection, formation flying, and air traffic control require collision avoidance. A key element of each of all these applications is position/velocity state estimation. Because a collision can often times be detected with a simple inexpensive accelerometer, this Note considers the addition of an accelerometer-based collision measurement to the state estimation process and provides evidence that the information associated with a negative collision measurement (i.e., a collision has not occurred) can provide useful state information and reduce state uncertainties.

A positive collision measurement (e.g., an abrupt change in an accelerometer output) will clearly provide some useful state information. During aircraft landing or powered descent, a positive collision measurement provides information about the altitude of the vehicle. During orbital rendezvous, a positive collision measurement provides information about the relative position of two spacecraft and indicates, at a minimum, that the two vehicles are in contact with each other. Although a positive collision measurement clearly has value, this is not the topic of this Note.

The absence of an abrupt change in acceleration, a negative collision measurement, is the topic of this Note. Because a negative collision is the absence of a measurement, one may initially believe that it cannot provide any useful information. However, consider the position covariance of an aircraft during landing. As the aircraft approaches the surface, the equiprobability ellipsoid begins to extend into the ground. A negative collision measurement, if processed properly, should eliminate the portion of the ellipsoid below the surface from consideration, move the mean or expected value of the altitude up away from the surface, and produce a smaller altitude error covariance.

Consider also the relative position error covariance ellipsoid associated with orbital rendezvous. In this case, a negative collision measurement should eliminate the portion of the error ellipsoid associated with the position and size of the spacecraft from consideration, move the mean position away from the spacecraft, and again produce a smaller position error covariance. If subsequent negative collision measurements are processed properly, the effect of coupled dynamics and state correlations may reduce the uncertainly further.

Because a negative collision measurement is the absence of a measurement, it can be considered negative information. Applications of negative information have been successfully incorporated and used in the estimation process. Koch [1] and Blanding et al. [2] investigated several radar tracking problems in which information associated with range and bearing measurements, as well as the absence of expected range and bearing measurements in jammed environments or low sensor resolution environments, is used to maintain better track of targets. Tishler and Vogt [3] also successfully used negative information in a cooperative multivehicle environment. They used the absence of expected radar measurements to aid in the collaborative perception of the environment. In both of these applications, negative information was derived from the absence of an expected traditional range and bearing measurement.

The negative collision measurements considered in this Note may also be considered negative information, but here the measurement is a nontraditional binary measurement (positive when a collision occurs and negative if a collision has not occurred), as opposed to the traditional range and bearing measurements considered in [1,3]. Although positive measurements will obviously provide very useful information, they will not be considered in this Note.

The objective of this Note is to conduct a preliminary assessment of the usefulness of negative collision measurements and determine whether or not negative collision measurements can provide real and useful information for improved position/velocity state estimation. In the future, a more detailed analysis will be required to fully assess the viability of negative collision measurements in real-time aerospace applications.

Because a collision measurement is a binary (positive or negative) random variable, a nonlinear sequential Monte Carlo "bootstrap filter" will be employed. A review of the bootstrap filter is provided next in Sec. II. In Sec. III, the bootstrap filter is applied to a constrained pendulum problem where collisions with side walls are possible. More complex satellite inspection and orbital rendezvous problems will be considered in Secs. IV and V. Final conclusions and remarks are presented in Sec. VI.

II. Bootstrap Filter

Although the applications considered next have linear time-invariant dynamics, a binary collision measurement cannot be treated with ordinary Kalman filtering techniques. Thus, to assess the usefulness of a negative collision measurement, a simple nonlinear sequential bootstrap filter is employed. The bootstrap filter is a simple particle filter in which the key idea is to eliminate particles having low importance weights and to multiply particles having high importance weights. After selecting an initial sample of states (particles) based upon the initial state probability density function, the known stochastic dynamics of the system are used to propagate the samples. When a measurement is received, the likelihood of each sample is evaluated and weighted appropriately. A subsequent resampling step eliminates particles with low importance and multiplies particles with high importance. The new sample set is then used to initialize the next propagate step. The mean and covariance of the samples can be computed at each step in the process. A nice overview of particle

Received 21 January 2013; revision received 16 September 2013; accepted for publication 13 August 2013; published online 26 March 2014.

*Associate Professor, Department of Mechanical and Aerospace Engineering. Senior Member AIAA.

†Professor and Holder of the Louis and Helen Rogow Chair in Aeronautical Engineering, Department of Aerospace Engineering.

filters is given by Oshman and Carmi [4], and additional details on particle filters and the bootstrap filter can be found in [5–8].

The general problem in this Note is to estimate the state of a linear time-invariant system with no process noise described in continuous time by

$$\dot{\boldsymbol{x}} = A\boldsymbol{x} \tag{1}$$

or in discrete time by

$$\boldsymbol{x}_{k+1} = \Phi\boldsymbol{x}_k \tag{2}$$

given only the initial probability density function (PDF) of the state $p(\boldsymbol{x}_0)$ and a sequence of scalar error-free collision measurements. Let Γ_k be a subset of the state space such that, if $\boldsymbol{x}_k$ is a member of Γ_k, a collision cannot occur at time t_k. The collision measurement can then be defined as

$$z_k(\boldsymbol{x}_k) = \begin{cases} -1 & \boldsymbol{x}_k \in \Gamma_k \\ +1 & \text{elsewhere} \end{cases} \tag{3}$$

Because there is no noise in the measurement equation, the likelihood probability mass function (PMF) is simply

$$\Pr\{z_k = -1|\boldsymbol{x}_k\} = \begin{cases} 1 & \boldsymbol{x}_k \in \Gamma_k \\ 0 & \text{elsewhere} \end{cases} \tag{4}$$

which says that, if the value of $\boldsymbol{x}_k$ is such that a collision at time t_k is not possible, then $z_k = -1$ with probability of one.

Given N random samples, $\boldsymbol{x}_0(i)$, $i = 1, \ldots, N$ from the initial a priori PDF $p(\boldsymbol{x}_0)$, the bootstrap filter will propagate the samples using the dynamics in Eqs. (1) or (2), and then update the samples using the likelihood PMF in Eq. (4).

Following Gordon et al. [7], the samples are first propagated forward to obtain N samples $\boldsymbol{x}^*_{k+1}(i)$ of the premeasurement PDF at time t_{k+1} using the dynamics model

$$\boldsymbol{x}^*_{k+1}(i) = \Phi\boldsymbol{x}_{k-1}(i), \qquad i = 1, \ldots, N \tag{5}$$

When a collision measurement is received, the unnormalized probability mass of each sample is determined as follows:

$$\tilde{q}_k(i) = \begin{cases} 1 & z_k(\boldsymbol{x}_k) = -1 \\ 0 & z_k(\boldsymbol{x}_k) = +1 \end{cases} \tag{6}$$

The $\tilde{q}_k(i)$ are normalized so that their sum equals one and then are used to define a discrete distribution over $\boldsymbol{x}^*_k(i)$, $i = 1, \ldots, N$ with probability mass $q_k(i)$ associated with sample i. In this way, a *negative* collision measurement removes all samples associated with a collision, $z_k(\boldsymbol{x}_k) = +1$. N new samples $\boldsymbol{x}_k(i)$, $i = 1, \ldots, N$ are then randomly selected from the new discrete distribution. Because the samples associated with a collision have been eliminated, the N new samples will contain multiplies of the samples that did not result in a collision.

The resampling stage is efficiently performed by first drawing a random sample u_i, $i = 1$, from a uniform distribution over $(0, 1]$. Then, u_i is used in Eq. (7) to determine the value of M and the first new sample $\boldsymbol{x}^*_k(M)$, where $1 \le M \le N$:

$$\sum_{j=0}^{M-1} q_k(j) < u_i \leqslant \sum_{j=0}^{M} q_k(j) \tag{7}$$

The procedure is repeated for $i = 2, \ldots, N$, so that each value of u_i determines a new value for M and the next new sample $\boldsymbol{x}^*_k(M)$, until N new samples are obtained. By definition $q_k(0) = 0$. The effect of Eq. (7) is to randomly multiply particles that have not resulted in a collision and eliminate particles that have resulted in a collision.

When the resampling procedure is complete, the new samples $\boldsymbol{x}_k(i)$, $i = 1, \ldots, N$ are propagated forward using Eq. (5) and the process continues. After each measurement, the mean and covariance of the N samples are computed according to

$$\hat{\boldsymbol{x}}_k = \frac{1}{N}\sum_{i=1}^{N} \boldsymbol{x}_k(i) \tag{8}$$

$$P_x = \frac{1}{N-1}\sum_{i=1}^{N} [\boldsymbol{x}_k(i) - \hat{\boldsymbol{x}}_k][\boldsymbol{x}_k(i) - \hat{\boldsymbol{x}}_k]^T \tag{9}$$

In the analysis that follows, the bootstrap filter and Eqs. (8) and (9) are used to compute the state estimates and state error covariances as a function of time, with and without negative collision measurements, using $N = 10,000$ samples. In the limit, as $N \to \infty$, the means and covariances will be exact. When negative measurements are unavailable, Eqs. (6) and (7) are omitted from the algorithm.

III. Constrained Pendulum Problem

To demonstrate the potential usefulness of a negative collision measurement, a constrained pendulum problem is first investigated. For small angles, the pendulum dynamics are governed by the simple linear differential equation

$$\ddot{\theta} = -\omega^2\theta, \qquad \omega = \sqrt{g/l)} = \text{constant}$$

where the largest possible angular deflection that can occur without a collision is θ_{lim}. In discrete time, the associated difference equations are

$$\theta_{k+1} = \theta_k \cos(\omega\Delta t) + \dot{\theta}_k \sin(\omega\Delta t)/\omega$$
$$\dot{\theta}_{k+1} = -\theta_k\omega \sin(\omega\Delta t) + \dot{\theta}_k \cos(\omega\Delta t)$$

If there are no measurements, and if the initial state is Gaussian and uncorrelated,

$$\theta_0 \sim N(\hat{\theta}_0, \sigma^2_{\theta_0}) \quad \dot{\theta}_0 \sim N(\hat{\dot{\theta}}_0, \sigma^2_{\dot{\theta}_0})$$

the time history of the state uncertainties can be determined analytically as follows:

$$\sigma^2_\theta(t) = \sigma^2_{\theta_0}\cos^2(\omega t) + \sigma^2_{\dot{\theta}_0}\sin^2(\omega t)/\omega^2 \tag{10}$$

$$\sigma^2_{\dot{\theta}}(t) = \omega^2\sigma^2_{\theta_0}\sin^2(\omega t) + \sigma^2_{\dot{\theta}_0}\cos^2(\omega t) \tag{11}$$

However, when a collision measurement is introduced

$$z_k(\theta_k, \dot{\theta}_k) = \begin{cases} -1, & |\theta_k| < \theta_{\text{lim}} \\ +1, & \text{elsewhere} \end{cases} \tag{12}$$

the problem becomes a nonlinear estimation problem with no known analytical solution. In this case, the bootstrap filter outlined in Sec. II can be employed to estimate the mean and state covariance of this problem using the likelihood PMF

$$\Pr\{z_k = -1|\theta_k, \dot{\theta}_k\} = \begin{cases} 1, & |\theta_k| < \theta_{\text{lim}} \\ 0, & \text{elsewhere} \end{cases} \tag{13}$$

As an example, consider a problem with $\theta_{\text{lim}} = 0.1$ rad, 20 collision measurements per cycle, and uncorrelated initial conditions:

$$\theta_0 \sim N(0.05 \text{ rad}, 0.05^2 \text{ rad}^2) \quad \dot{\theta}_0 \sim N(0.75 \text{ rad/s}, 0.2^2 \text{ rad}^2/\text{s}^2)$$

If a collision occurs, the position is immediately known (i.e., $\theta = \pm\theta_{\text{lim}}$) (the $\pm$ ambiguity is not a concern here). However, if a

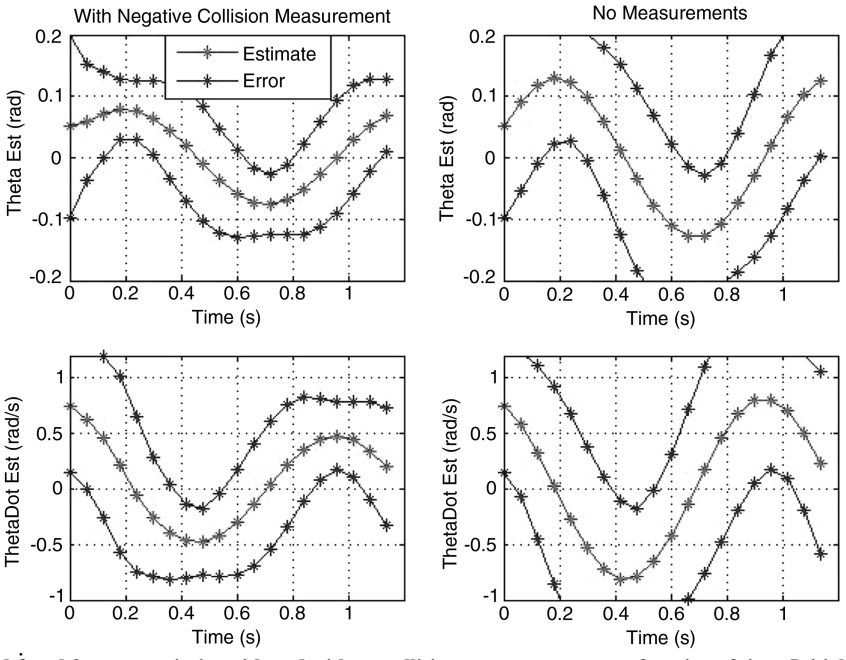

Fig. 1 Estimates of θ and $\dot{\theta}$ and 3-σ uncertainties with and without collision measurements as a function of time. Initial conditions are Gaussian.

collision does not occur, the pendulum will swing freely, and all the collision measurements will be negative. In this case, the bootstrap filter shows that negative collision measurements will improve the uncertainty in the state estimate. Figure 1 shows the time history of the filter state estimates and the 3-σ state uncertainties with collision measurements (left) and without collision measurements (right). The middle curves show the state estimates given by Eq. (8) and the top/bottom curves show the 3-σ uncertainty bounds given by Eq. (9). Because the problem without collision measurements is linear, the results of the bootstrap filter were validated using Eqs. (10) and (11). The data in Fig. 1 clearly show a flattening and tightening of the estimation errors when negative collision measurements are employed, an improvement seen without an actual collision or any apparent real measurements. Nonetheless, negative collision measurements do provide information. Fundamentally, the source of this information is the collision boundary in the state space. This will be seen more clearly in Secs. IV and V.

The initial Gaussian statistics used earlier are arguably not very realistic because it is physically impossible for the pendulum to be outside the θ_{lim} bound. A more accurate approach is to assume the initial PDF is uniform. Using a uniform distribution with support,

$$0.0 \le \theta_0 \le 0.1 \text{ rad} \quad 0.55 \le \dot{\theta}_0 < 0.95 \text{ rad/s}$$

a bootstrap filter was employed with and without the collision measurement. Figure 2 shows the resulting time histories of the filter state estimates along with the 3-σ state uncertainty bounds. Here, the negative collision measurements even more clearly improve the state estimates, even though a collision has not occurred. These examples provide the evidence needed to justify further investigation.

It is noted that, for a simple pendulum, a collision can be predicted quite easily using conservation of energy methods. Any combination of θ_0 and $\dot{\theta}_0$ that satisfies the relation

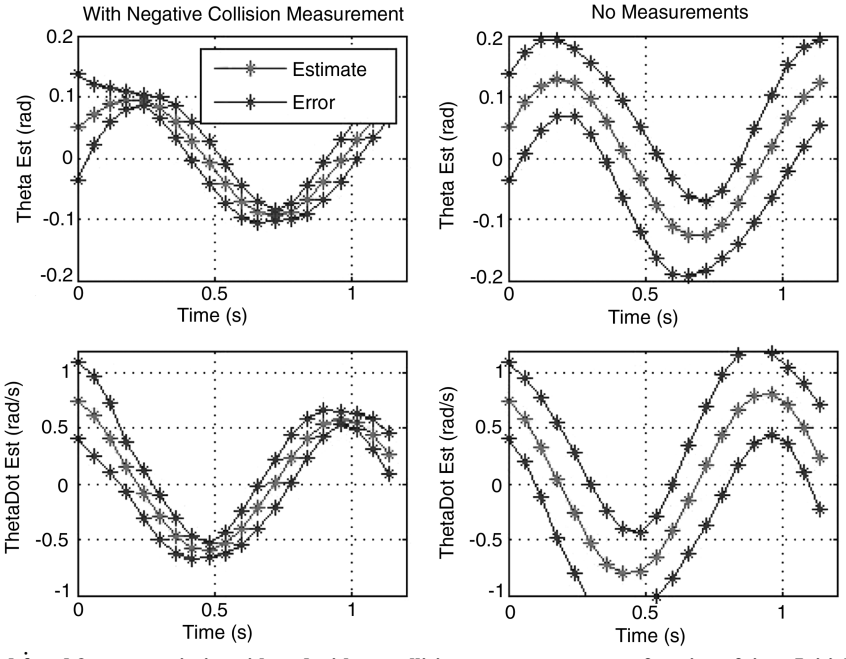

Fig. 2 Estimates of θ and $\dot{\theta}$ and 3-σ uncertainties with and without collision measurements as a function of time. Initial conditions are uniform.

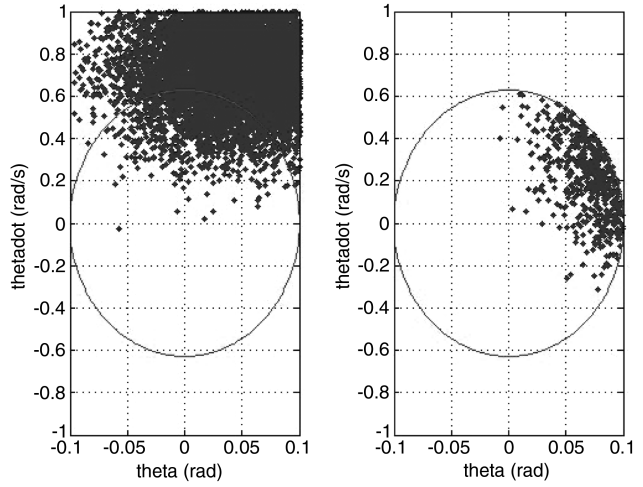

Fig. 3 Initial Gaussian (left) and final (right) state PDF after processing negative collision measurements. The curve, Eq. (14), bounds the states that will not collide with the side walls.

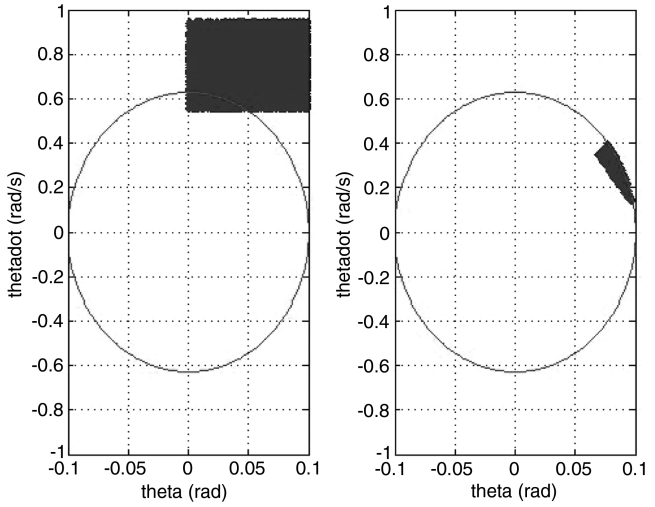

Fig. 4 Initial uniform (left) and final (right) state PDF after processing negative collision measurements. The curve, Eq. (14), bounds the states that will not collide with the side walls.

$$\frac{1}{2}\omega^2\theta_{\lim}^2 < \frac{1}{2}\dot{\theta}_0^2 + \frac{1}{2}\omega^2\theta_0^2 \tag{14}$$

will result in a collision. This energy-based collision constraint is shown in Figs. 3 and 4 along with the initial and final PDFs for the two preceding pendulum problems. In this simple case, Eq. (14) could have been used to cull or trim the initial state PDF to obtain the same results as the bootstrap filter. However, in more complex problems, such as formation flying or orbital rendezvous and docking, there is no known simple efficient way to trim the state PDF by predicting collisions, but a nonlinear estimation algorithm can produce the same results.

IV. Satellite Inspection Problem

In this example, a satellite inspection problem will be investigated. For simplicity, it is assumed that an inspector spacecraft and some other space object are in the same orbit plane and in nearly circular orbits. The relative motion can be described by the in-plane components of the Clohessy–Wiltshire equations [9],

$$\ddot{x} = -2\omega\dot{y} \tag{15}$$

$$\ddot{y} = 3\omega^2 y + 2\omega\dot{x} \tag{16}$$

where x is the downrange relative position in the direction of the inertial velocity, y is the relative altitude in the radial direction, and ω is the orbit frequency. These second-order linear coupled differential equations can also be written in discrete time using the state transition matrix.

$$x_{k+1} = 6(\sin\omega\Delta t - \omega t)y_k + x_k - \frac{2}{\omega}(1-\cos\omega\Delta t)\dot{y}_k + \frac{4\sin\omega\Delta t - 3\omega\Delta t}{\omega}\dot{x}_k \tag{17}$$

$$y_{k+1} = (4-3\cos\omega\Delta t)y_k + \frac{\sin\omega\Delta t}{\omega}\dot{y}_k + \frac{2}{\omega}(1-\cos\omega\Delta t)\dot{x}_k \tag{18}$$

$$\dot{x}_{k+1} = -6\omega(1-\cos\omega\Delta t)y_k - 2(\sin\omega\Delta t)\dot{y}_k + (4\cos\omega\Delta t - 3)\dot{x}_k \tag{19}$$

$$\dot{y}_{k+1} = (3\omega\sin\omega\Delta t)y_k + (\cos\omega\Delta t)\dot{y}_k + 2(\sin\omega\Delta t)\dot{x}_k \tag{20}$$

For orbital rendezvous, the error-free collision measurement is given by

$$z_k(x_k, y_k, \dot{x}_k, \dot{y}_k) = \begin{cases} -1, & \|x_k\| > r_{\lim} \quad \text{and} \quad \|y_k\| > r_{\lim} \\ +1, & \text{otherwise} \end{cases} \tag{21}$$

and the conditional PMF is given by

$$\Pr\{z_k = -1 | x_k, y_k, \dot{x}_k, \dot{y}_k\} = \begin{cases} 1, & \|x_k\| > r_{\lim} \quad \text{and} \quad \|y_k\| > r_{\lim} \\ 0, & \text{elsewhere} \end{cases} \tag{22}$$

where $r_{\lim}$ is the minimum distance the two vehicles can approach each other without colliding. In this example, both spacecraft are modeled as simple square objects. The minimum distance $r_{\lim}$ is the sum of the sides of the two squares divided by two.

Two inspection missions are considered and shown in local-vertical/local-horizontal (LVLH) coordinates in Figs. 5 and 6. The first is a flyby inspection, in which the inspector is placed on a coelliptic trajectory above a space object. The second is circumnavigation inspection (football orbit) where the inspector orbit has the same orbital energy as the space object, but a slightly different eccentricity. Woffinden [10] and Woffinden and Geller [11] describe these two scenarios in great detail.

The bootstrap filter described by Eqs. (5–9) was applied to this problem using the dynamics in Eqs. (17–20) and the conditional PMF given by Eq. (22). In this example, all collision measurements, 15 measurements per orbit period, were negative. The spacecraft were placed in near-circular low Earth orbits (LEOs) and the analysis was conducted for 1.5 orbits with and without collision measurements.

In satellite inspection missions, the 3-σ extent of the initial PDF is typically less than the distance between the inspector and the space object to ensure a collision-free environment. With this type of initial condition, negative collision measurements are found to be ineffective in reducing the covariance of the relative position vector for a wide array of initial test conditions. Even when the 3-σ extent of the PDF extends slightly into the space object as shown in Fig. 7, the effect of negative collision measurements on the position estimates and covariance is negligible. The time histories of the state estimates and 3-σ uncertainty for a particular inspection scenario are shown in Fig. 8. There are no noticeable differences between the results with collision measurements and the results without collision measurements. These results indicate that the source of the information from a negative collision measurement comes from the collision boundary in the state space. When the boundary does not

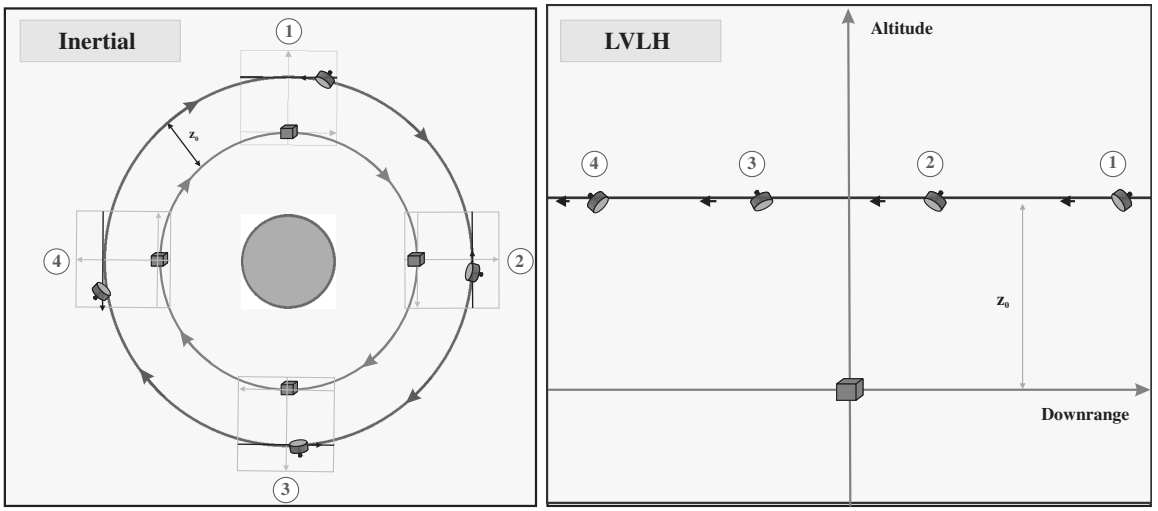

Fig. 5 Flyby, coelliptic approach scenario. Inspection satellite is initially 10 m above and 50 m behind the space object.

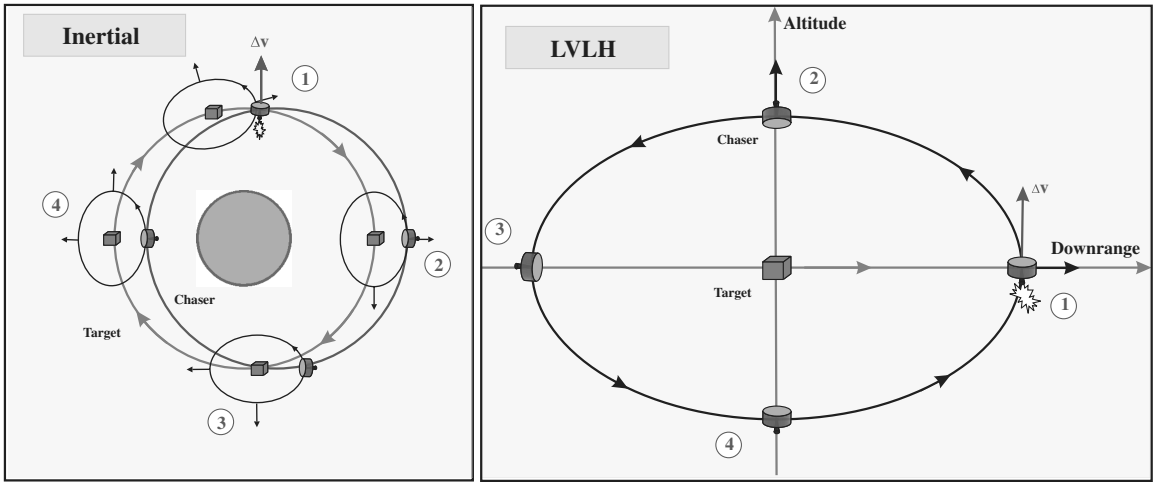

Fig. 6 Circumnavigation football orbit scenario. Ellipse semimajor axis is 50 m. Inspection satellite is initially 50 m behind and 0 m above the space object.

extend significantly into the state PDF in a statistical sense, the state covariance cannot be reduced.

The bootstrap filter was also applied to several satellite inspection scenarios where known open-loop maneuvers were applied to the inspector to change its path. The measurement rate was again 15 negative collision measurements per orbit. This also produced little or no improvement in the state uncertainties. Even when the inspector spacecraft was commanded in an open-loop fashion to maneuver along a linear path toward the space object, the test results with negative collision measurements differed little from the no-measurement cases, except when the distance between the inspector and the space object became so small that a collision was likely.

Because the dynamics of the satellite inspection problem are linear and Gaussian, all results without collision measurements were validated using ordinary linear stochastic systems theory [12] (i.e., the bootstrap filter results without collision measurements were reproduced by simply propagating the initial state covariance forward using the known linear dynamics model).

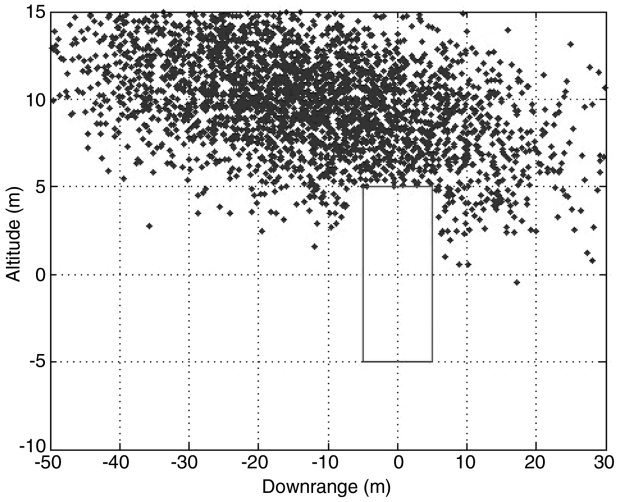

Fig. 7 Downrange/altitude PDF during a flyby, coelliptic approach inspection mission. Box represents the space object being inspected.

V. Rendezvous and Docking

Examining the inspection mission results, it becomes clear that, unless the state PDF extends significantly into the space object with sufficient probability density, the collision measurements are ineffective. And so, instead of considering applications where collisions are undesirable, an application with a desirable collision (rendezvous and docking) is warranted.

In this scenario, a chaser spacecraft moves along the local horizontal with constant velocity in the downrange direction toward a docking target with near-zero relative altitude, as illustrated in Fig. 9. The chaser and target are initialized in circular LEO orbits with an initial separation of 5 m and a constant closing velocity of -1 cm/s.

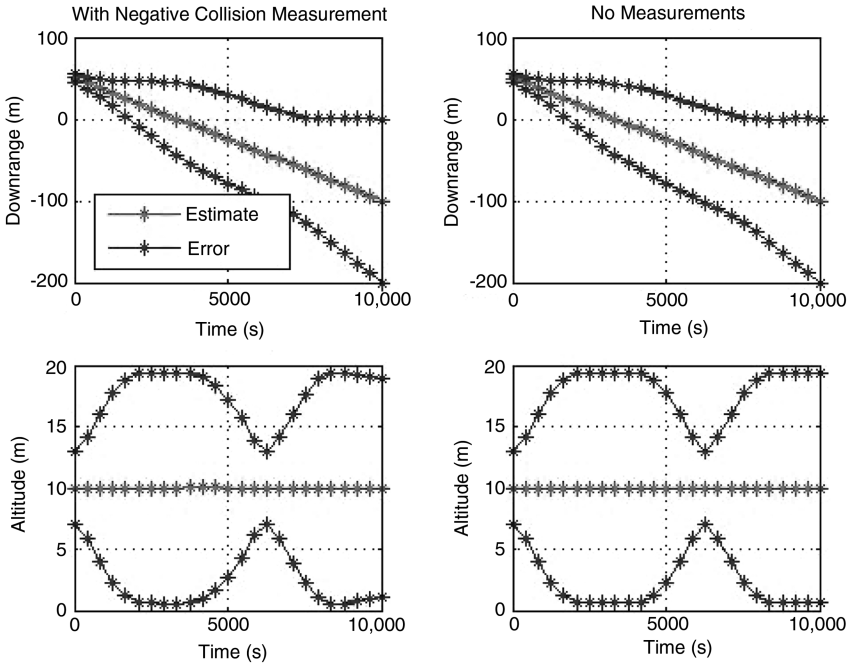

Fig. 8 Flyby mission downrange/altitude estimates and 3-σ uncertainty with negative collision measurements (left) and without measurements (right).

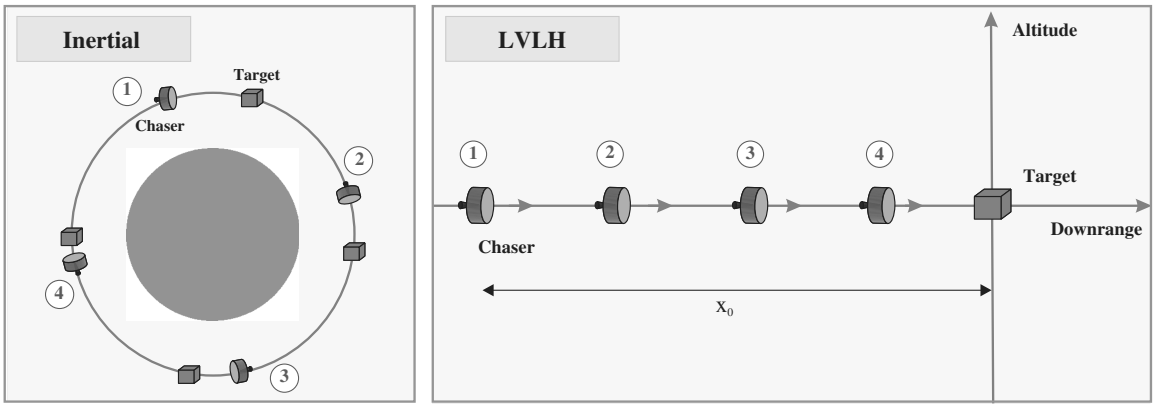

Fig. 9 *V*-bar approach scenario for rendezvous and docking. Initial distance to nominal contact is 5 m and approach velocity is −1 cm/s.

The addition of a small radial thrust acceleration to the dynamics in Eqs. (17–20) is required to implement this approach.

Using the new dynamics and the original conditional PDF in Eq. (22), the bootstrap filter was used to estimate the relative position and relative velocity with and without collision measurements. For convenience, the measurement rate was once every 100 s, though faster measurement rates had little effect on the final results. The initial state and state covariance are given below. Note the high negative correlation between x_0 and $\dot{y}_0$, and between y_0 and $\dot{x}_0$. This is typical of orbiting spacecraft and is due to the nature of orbital dynamics [13]:

$$\hat{X}_0 = \begin{bmatrix} \hat{x}_0 \\ \hat{y}_0 \\ \hat{\dot{x}}_0 \\ \hat{\dot{y}}_0 \end{bmatrix} = \begin{bmatrix} 10\ \text{m} \\ 0\ \text{m} \\ -5\ \text{mm/s} \\ 0\ \text{mm/s} \end{bmatrix}$$

$$P_0 = \begin{bmatrix} 1.0^2\ \text{m}^2 & 0 & 0 & -0.98\ \text{m} \cdot \text{mm/s} \\ 0 & 0.1^2\ \text{m}^2 & -0.098\ \text{m} \cdot \text{mm/s} & 0 \\ 0 & -0.098\ \text{m} \cdot \text{mm/s} & 1.0\ \text{mm}^2/\text{s}^2 & 0 \\ -0.98\ \text{m} \cdot \text{mm/s} & 0 & 0 & 0.1\ \text{mm}^2/\text{s}^2 \end{bmatrix}$$

Snapshots of the time evolution of the position PDF at times $t = 0$, 400, 700, and 900 s are shown in Fig. 10 (progressing from right to left). Notice how a delay in the docking (and more negative collision measurements) forces the position estimate downward. This is due to the preceding correlations (i.e., positive altitude error is correlated to negative downrange velocity). The source of the information that allows this to happen is in the collision boundary. Notice how the collision boundary in the state space reshapes the statistical distribution of the state, which in turn alters the mean and variance of the state.

The time histories of the filter state estimates along with the 3-σ state uncertainty bounds are given in Fig. 11. The results show that

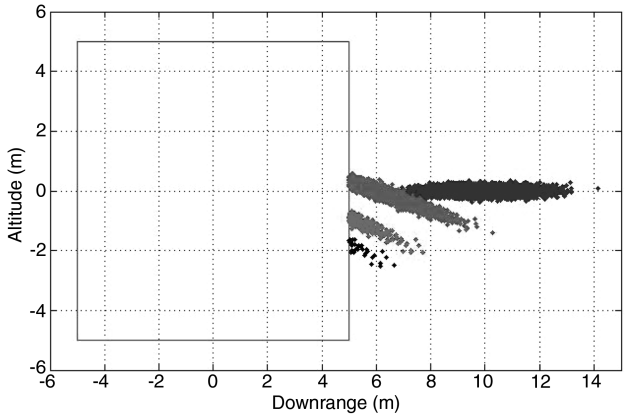

Fig. 10 Downrange and attitude PDF as a function of time: $t = 0$, 400, 700, and 900 s.

the position covariance is reduced by a factor of approximately 2.5 when negative collision measurements are processed. The 3-σ downrange errors are reduced from 5 to 2 m, and the 3-σ altitude errors are reduced from 2.5 to 1 m. In addition, the altitude estimates are properly driven to negative values. This result is merely a reflection of the initial state correlations (a delayed collision implies a positive perturbation to the downrange velocity). This, in turn, results in a negative perturbation to the altitude due to the negative correlations. Because the dynamics of this problem are again linear and Gaussian, the bootstrap filter results without collision measurements were validated using ordinary linear stochastic systems theory [12].

VI. Conclusions

A preliminary assessment of the usefulness of negative collision measurements has been conducted. From the above analysis, it can be concluded that negative collision measurements can provide real and potentially useful information for improved position/velocity state estimation. Fundamentally, the source of the information comes from the collision boundary in the state space. When the boundary extends significantly into the state PDF in a statistical sense, the state covariance can be reduced. This, in turn, affects subsequent state estimates.

For satellite inspection missions, where collisions are undesirable and the constraint boundary does not extend significantly into the state PDF, the effect of negative collision measurements on the position covariance differs little from the case with no negative collisions measurements. For rendezvous and docking, however, results show that the position covariance can be significantly reduced and useful state updates can be obtained by processing negative collision measurements.

Acknowledgments

This research was conducted with support and funding from the Lady Davis Fellowship Trust and the Asher Space Research Fund.

References

[1] Koch, W., "On Negative Information in Tracking and Sensor Data Fusion: Discussion of Selected Examples," *Proceedings of the Seventh International Conference on Information Fusion*, IEEE Publ., Piscataway, NJ, 2004, pp. 91–98.

[2] Blanding, W., Koch, W., and Nickel, U., "Tracking Through Jamming Using Negative Information," *9th International Conference on Information Fusion*, Florence, Italy, IEEE Publ., Piscataway, NJ, 2006.

[3] Tischler, K., and Vogt, H., "Data Fusion Approach for the Integration of Negative Information," *Proceedings of the 10th International Conference on Information Fusion*, IEEE Publ., Piscataway, NJ, 2007, pp. 1–7.

[4] Oshman, Y., and Carmi, A., "Attitude Estimation from Vector Observations Using Genetic-Algorithm-Embedded Quaternion Particle Filter," *Journal of Guidance, Control, and Dynamics*, Vol. 29, No. 4, 2006, pp. 879–891. doi:10.2514/1.17951

[5] Carmi, A., and Oshman, Y., "Fast Particle Filtering for Attitude and Angular-Rate Estimation from Vector Observations," *Journal of Guidance, Control, and Dynamics*, Vol. 32, No. 1, 2009, pp. 70–77. doi:10.2514/1.36979

[6] Carmi, A., and Oshman, Y., "Adaptive Particle Filtering for Spacecraft Attitude Estimation from Vector Observations," *Journal of Guidance, Control, and Dynamics*, Vol. 32, No. 1, 2009, pp. 232–241. doi:10.2514/1.35878

[7] Gordon, N. J., Salmond, D. J., and Smith, A. F. M., "Novel Approach to Nonlinear/Non-Gaussian Bayesian State Estimation," *IEE Proceedings-F*, Vol. 140, No. 2, 1993, pp. 107–113.

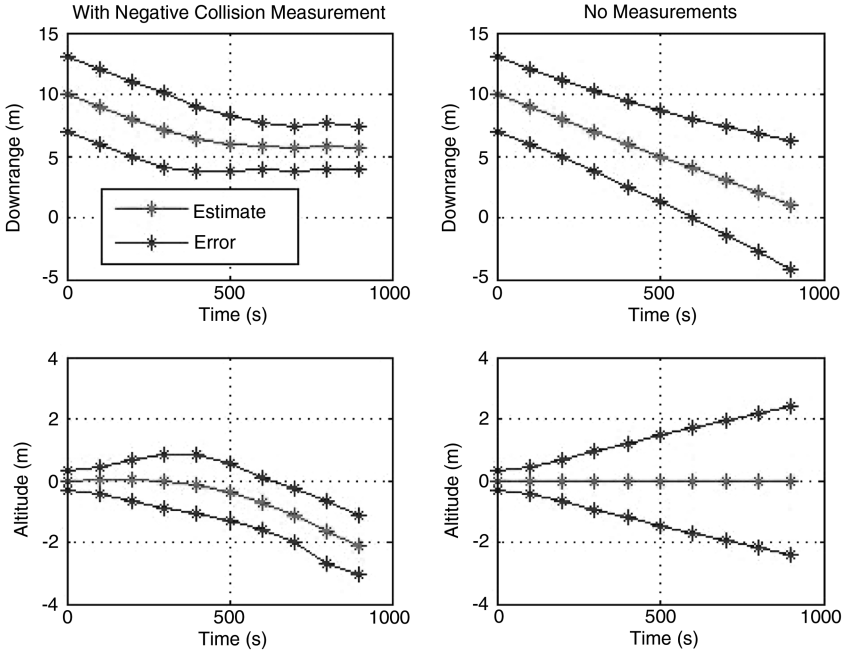

Fig. 11 Downrange and attitude estimates and 3-σ uncertainty bounds as a function of time with negative collision measurements (left) and without collision measurements (right).

[8] Doucet, A., de Freitas, N., and Gordon, N., *Sequential Monte Carlo Methods in Practice*, Springer, New York, 2011, pp. 10–12.
[9] Vallado, D. A., *Fundamentals of Astrodynamics and Applications*, Kluwer Academic, Norwell, MA, 2004, pp. 374–380.
[10] Woffinden, D., Angles-Only Navigation for Autonomous Orbital Rendezvous, Ph.D. Thesis, Utah State Univ., Logan, UT, Aug. 2008.
[11] Woffinden, D. C., and Geller, D. K., "Observability Criteria for Angles-Only Navigation," *IEEE Transactions on Aerospace and Electronic Systems*, Vol. 45, No. 3, 2009, pp. 1194–1208. doi:10.1109/TAES.2009.5259193
[12] Maybeck, P. S., *Stochastic Models, Estimation and Control, Volume 1*, Academic Press, New York, 1994, pp. 163–170.
[13] Lear, W. M., "Kalman Filtering Techniques," NASA TR-JSC-20688, 1985.